

Luminescent Organogold(III) Complexes with Long-Lived Triplet Excited States for Light-Induced Oxidative C–H Bond Functionalization and Hydrogen Production**

Wai-Pong To, Glenna So-Ming Tong, Wei Lu, Chensheng Ma, Jia Liu, Andy Lok-Fung Chow, and Chi-Ming Che*

Transition-metal complexes with high-energy, long-lived, and highly emissive triplet excited states have profound applications in photocatalysis^[1] and biosensing.^[2] In this regard, luminescent gold(III) complexes have recently received much interest as complementary species to their isoelectronic platinum(II) congeners.^[3] Although there have been considerable efforts to develop organogold(III) photochemistry since the 1990s,^[4] cyclometalated gold(III) complexes that are highly emissive in fluid solutions are still sparse.^[5,6] The high electrophilicity of gold(III) ion renders the unoccupied $d\sigma^*$ ($d_{x^2-y^2}$) orbital low-lying and thus the low-energy ligand-to-metal charge transfer (LMCT) excited state(s) close to the emissive intraligand excited states, leading to effective luminescence quenching.^[5a] To increase the luminescence efficiency of gold(III) complexes, strong-field ligands are desired to push the $d\sigma^*$ orbital to higher-lying energy. The incorporation of a strong σ -donating auxiliary ligand L, such as an acetylide or an N-heterocyclic carbene (NHC), to the bis-cyclometalated $[\text{Au}^{\text{III}}(\text{C}^{\wedge}\text{N}^{\wedge}\text{C})\text{L}]^+$ ($\text{HC}^{\wedge}\text{N}^{\wedge}\text{CH} = 2,6$ -diphenylpyridine) system^[6a] was found to be successful, resulting in phosphorescence in solutions with emission quantum yields of up to 1.0 % and lifetimes up to 0.6 μs ,^[6b–g] indicating fast nonradiative decay ($k_{\text{nr}} \approx 10^6$ – 10^7 s^{-1}) and moderate radiative decay ($k_{\text{r}} \approx 10^3$ – 10^4 s^{-1}).

Herein we present the photophysical and photocatalytic properties of two novel gold(III) complexes bearing an extended π -conjugated bis-cyclometalated ligand (Figure 1 a). A π -extension in bis-cyclometalated ligand is anticipated to

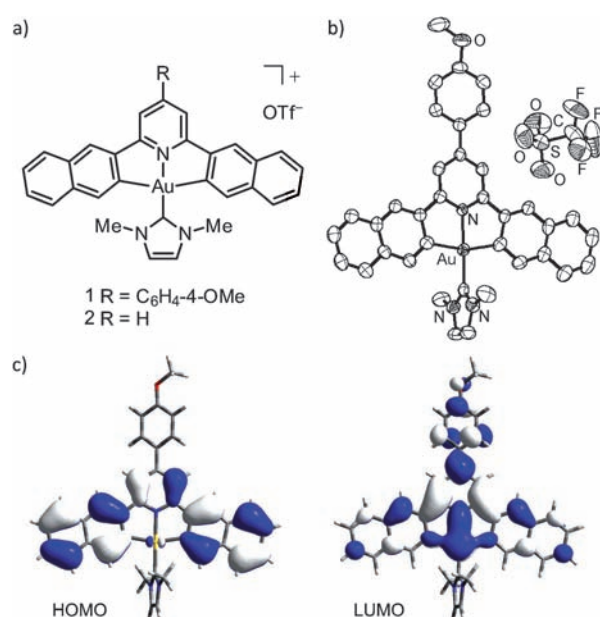


Figure 1. a) Chemical structure of **1** and **2**; b) ORTEP of **1** with ellipsoids set at 50% probability and hydrogen atoms omitted for clarity; c) Calculated HOMO and LUMO of **1**.

enhance radiative decay by increasing the transition dipole (μ) and oscillator strength (f) of the $S_0 \rightarrow S_1$ transition whereas suppressing nonradiative decay by decreasing the structural excited-state distortion. Indeed, emissive excited states with lifetimes of 282 and 506 μs in solutions at room temperature were recorded with these two complexes and, to our best knowledge, unprecedented for luminescent organogold(III) complexes. We also demonstrated that these long-lived triplet intraligand excited states can be harnessed to catalyze oxidative functionalization of secondary and tertiary benzylic amines and homogeneous hydrogen production from a water/acetonitrile mixture.

Details for the synthesis and characterization of $[\text{Au}^{\text{III}}(\text{R}-\text{C}_{\text{np}}^{\wedge}\text{N}^{\wedge}\text{C}_{\text{np}})(\text{NHC})](\text{OTf})$ ($\text{R}-\text{HC}_{\text{np}}^{\wedge}\text{N}^{\wedge}\text{C}_{\text{np}}\text{H} = 4\text{-R-2,6-dinaphthalen-2-yl-pyridine}$; $\text{R} = \text{C}_6\text{H}_4\text{-4-OCH}_3$ (**1**), and $\text{R} = \text{H}$ (**2**); $\text{NHC} = 1,3$ -dimethylimidazol-2-ylidene) are given in the Supporting Information. The structure of **1** has been confirmed by single-crystal X-ray crystallography.^[7] As shown in Figure 1 b, the $(\text{C}_{\text{np}}^{\wedge}\text{N}^{\wedge}\text{C}_{\text{np}})$ ligand and gold atom are in a coplanar geometry, revealing the structural rigidity of this complex. The dihedral angle between the $\text{Au}(\text{C}_{\text{np}}^{\wedge}\text{N}^{\wedge}\text{C}_{\text{np}})$

[*] W.-P. To, Dr. G. S.-M. Tong, Dr. W. Lu, C. Ma, Dr. J. Liu, Dr. A. L.-F. Chow, Prof. Dr. C.-M. Che
State Key Laboratory of Synthetic Chemistry, Institute of Molecular Functional Materials, HKU-CAS Joint Laboratory on New Materials, and
Department of Chemistry, The University of Hong Kong
Pokfulam Road, Hong Kong (China)
E-mail: cmche@hku.hk

Dr. W. Lu
Department of Chemistry
South University of Science and Technology of China
1088 Xueyuan Boulevard, Shenzhen, Guangdong 518055 (China)

[**] This work was supported by the Hong Kong Research Grants Council (HKU 7008/09P and AoE/P-03/08), NSFC/RGC Joint Research Scheme (N_HKU 752/08), and the CAS-Croucher Funding Scheme for Joint Laboratories. We thank Dr. Yong Chen for solving the crystal structure.

Supporting information for this article is available on the WWW under <http://dx.doi.org/10.1002/ange.201108080>.

coordination plane and the NHC ligand is about 89°, which is presumably due to the steric hindrance between the two methyl groups and the two naphthalenyl hydrogen atoms close to the gold atom.

Density functional theory (DFT) and time-dependent DFT (TDDFT) calculations have been performed on both the prototype complexes $[\text{Au}^{\text{III}}(\text{C}^{\wedge}\text{N}^{\wedge}\text{C})(\text{NHC})]^+$ and $[\text{Au}^{\text{III}}(\text{R-C}_{\text{np}}^{\wedge}\text{N}^{\wedge}\text{C}_{\text{np}})(\text{NHC})]^+$ (**1**⁺) at their respective optimized S_0 ground state and T_1 excited state geometries. The oscillator strengths (f) of the low-lying singlet excited states from which the triplet excited state can borrow intensity is larger in **1**⁺ and the change in bond lengths between the singlet ground state (S_0) and the first triplet excited state (T_1) is smaller for **1**⁺ (see Supporting Information). The singlet–triplet energy gap at the Franck–Condon state is smaller in **1**⁺ (1000–2500 cm^{-1} , depending on excitation wavelength) than in $[\text{Au}^{\text{III}}(\text{C}^{\wedge}\text{N}^{\wedge}\text{C})(\text{NHC})]^+$ (ca. 3600 cm^{-1}). Accordingly, **1**⁺ has a faster inter-system crossing (ISC) rate and higher triplet quantum yield. At the Franck–Condon state, there is a minor contribution of ligand-to-metal charge-transfer (LMCT) character in the low-lying singlet excited states of $[\text{Au}^{\text{III}}(\text{C}^{\wedge}\text{N}^{\wedge}\text{C})(\text{NHC})]^+$ but none in those of **1**⁺. Thus, it is expected that **1**⁺ has a slower nonradiative decay rate than $[\text{Au}^{\text{III}}(\text{C}^{\wedge}\text{N}^{\wedge}\text{C})(\text{NHC})]^+$. Indeed, the nonradiative decay of **1**⁺ is more than 300-fold slower than that of $[\text{Au}^{\text{III}}(\text{C}^{\wedge}\text{N}^{\wedge}\text{C})(\text{NHC})]^+$ (see below).

The low-energy absorption bands of **1** and **2** in dichloromethane with λ_{max} at 403 nm and 402 nm ($\epsilon_{\text{max}} \approx 1.7\text{--}2.6 \times 10^4 \text{ dm}^3 \text{ mol}^{-1} \text{ cm}^{-1}$) are assigned to intra-ligand transitions localized at the $(\text{R-C}_{\text{np}}^{\wedge}\text{N}^{\wedge}\text{C}_{\text{np}})$ ligand. Dual emission bands with λ_{max} at 420 and 520 ± 1 nm are found in the emission spectra of both **1** and **2** in degassed dichloromethane at a complex concentration of $1.0 \times 10^{-5} \text{ mol dm}^{-3}$ at 298 K (Figure 2a). The vibronically structured low-energy emission band reveals a spacing of about 1400 cm^{-1} corresponding to stretching frequencies of the dinaphthalen-2-yl-pyridine moiety. The quantum yields of the lower-energy emission are 11.4 % and 5.5 % for **1** and **2**, respectively; the lifetimes of the lower-energy (519–521 nm) emission bands are 506 μs for **1** and 282 μs for **2**. Both the excitation spectra monitored at $\lambda_{\text{em}} = 420$ nm and 519–521 nm show well-resolved vibronic structures with λ_{max} at 402–403 nm, which is identical to that of the absorption spectrum (Figure 2a). There is negligible solvent effect on the emission spectra of **1** and **2**. Upon excitation at 380 nm, femtosecond time-resolved emission measurements with dichloromethane solutions of **1** and **2** established that the lifetime of the higher-energy emission (420 nm) is in the picosecond region (3.3 ps for **1** and 3.7 ps for **2**; see Supporting Information) and the excited states of which rapidly decay by intersystem crossing with a rate constant estimated to be about $3 \times 10^{11} \text{ s}^{-1}$ to the triplet emissive excited state having the emission λ_{max} at about 520 nm. We thus assign the high- and low-energy emission bands to the respective prompt fluorescence and phosphorescence from metal-perturbed intraligand excited state.

There is a more than 100-fold decrease in emission intensity at 519–521 nm upon exposure of solutions of **1** and **2** to air. The 420 nm emission band is not changed during the O_2 diffusion process (Figure 2b). Given the long emission lifetimes of 506 and 282 μs , it is not surprising to find the

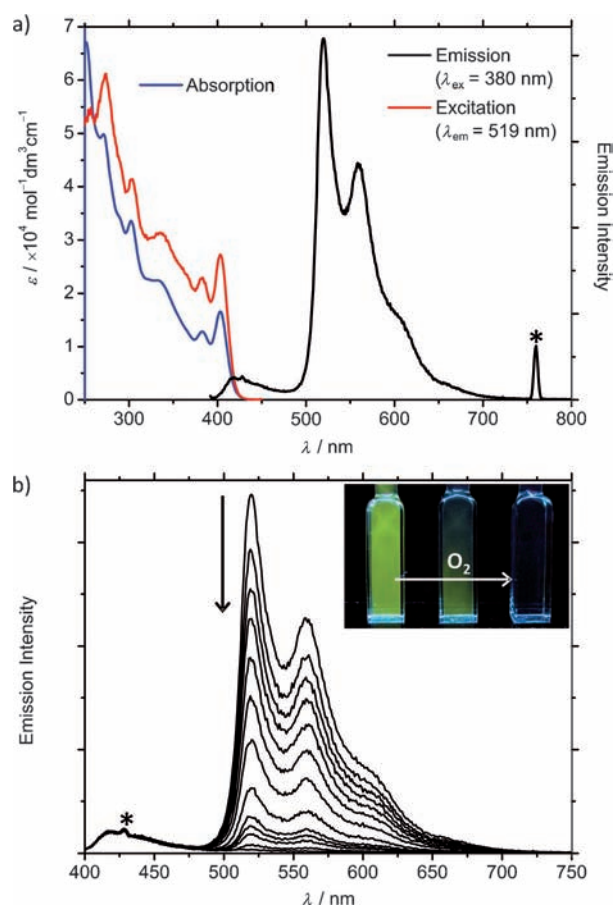


Figure 2. a) Electronic absorption, emission, and excitation spectra of **1** (concentration ca. $1.0 \times 10^{-5} \text{ mol dm}^{-3}$) in degassed CH_2Cl_2 at room temperature. The asterisk indicates a second-order transmission of the 380 nm excitation. b) Emission traces showing the decrease of emission intensity upon slow diffusion of air into a thoroughly degassed dichloromethane solution of **1**. Only 1 % of the emission intensity at 519 nm was retained after exposure to air. Excitation wavelength: 380 nm; asterisk indicates an instrumental artifact. Inset: the air diffusion process under a 365 nm lamp.

significant O_2 quenching effect on the emission intensity at 519–521 nm. The sensitivity of the emission of **2** towards oxygen can be harnessed to visualize the living cells (see video in Supporting Information). When nitrogen was blown over the living cells incubated with **2** in buffer solution, these cells became yellowish green upon illumination under a fluorescent microscope. This reveals that **2** can be taken into the living cells and serves as an O_2 sensor inside.

The high emission quantum yields and long-lived triplet excited states render **1** and **2** good candidates for photochemical reactions. By employing the electrochemical data plus the spectroscopic measurements, we estimated the excited-state potential of **1** by using the following equation: $E(*\mathbf{1}^{+/0}) = E(\mathbf{1}^{+/0}) + E_{0,0}(\mathbf{1}^+)$. The cyclic voltammogram of **1** reveals the first quasi-reversible one-electron reduction wave [$E(\mathbf{1}^+/\mathbf{1}^0)$, ($i_{\text{pc}}/i_{\text{pa}} \approx 1$) at -1.73 V vs. $\text{Cp}_2\text{Fe}^{+/0}$ (-1.04 V vs. NHE)]. The 0–0 transition energy of **1**, $E_{0,0}(\mathbf{1}^+)$, can be estimated from the onset of the triplet emission band, which occurs at about 500 nm (2.48 eV). Thus $E(*\mathbf{1}^{+/0})$ is estimated

to be about 0.75 V vs. $\text{Cp}_2\text{Fe}^{+/0}$ (1.43 V vs. NHE), signifying that **1** is a powerful photooxidant. Complex **1** was chosen in the present study to test for its photocatalytic activities.

Oxidation of secondary amines to imines and α -substitution of tertiary amines have important applications in organic synthesis.^[8] In the presence of oxygen, **1** was found to catalyze oxidation of secondary amines under light irradiation at room temperature. As summarized in Table 1, secondary benzyl

Table 1: Conversion and yield of oxidation of secondary amines to imines by complex **1**.^[a]

Entry	Substrate	R ¹	R ²	Product	Conversion, yield [%]
1	3 a	H	<i>t</i> Bu	4 a	100, 98
2	3 b	Me-4	<i>t</i> Bu	4 b	100, 98
3	3 c	OMe-4	<i>t</i> Bu	4 c	100, 97
4	3 d	(OMe) ₂ -3,4	<i>t</i> Bu	4 d	100, 94
5	3 e	F-4	<i>t</i> Bu	4 e	100, 96
6	3 f	Cl-4	<i>t</i> Bu	4 f	100, 97
7	3 g	H	Bn	4 g	100, 98
8	3 h	H	<i>i</i> Pr	4 h	100, 89

[a] The substrate (0.107 mmol) and catalyst **1** were dissolved in 1.6 mL CH_3CN . Solvent-saturated O_2 was bubbled into the solution and light ($\lambda > 385$ nm) was focused in front of the quartz cell. After 2.5 h, the solvent was evaporated and the residue was subjected to ^1H NMR analysis. Conversions and yields were calculated on the basis of the consumption of the substrates.

amines with a variety of functional groups (R^1 and R^2) can be converted to imines efficiently in the presence of **1**; light irradiation and oxygen were used together as the oxidant. Notably, all entries reached 100% conversion with excellent product yields (89–98%), but only 0.15 mol % of **1** as catalyst and a short irradiation time of 2.5 h were required. Singlet oxygen sensitized from the triplet state of **1** is suggested to be an active oxidant in this reaction.

We also turned our attention to the oxidative cyanation of tertiary amines, such as *N*-aryltetrahydroisoquinoline (Table 2). When *N*-phenyl-1,2,3,4-tetrahydroisoquinoline is used, the α -C–H bond reacts with singlet oxygen to give iminium ions as the intermediate. The iminium ion is unstable and rapidly reacts with nucleophiles to give the corresponding α -substituted products. In this work, all of the *N*-aryl tetrahydroisoquinoline substrates reacted with sodium cyanide in the presence of acetic acid to give the products in 82–92% yields after 1.5 h of irradiation ($\lambda > 385$ nm). This reaction is tolerable to a variety of substituents *R* on the *N*-aryl group. The addition of acetic acid is crucial, as the product yield obtained without acetic acid is significantly lower. Murahashi and co-workers have recently reported that the oxidative cyanation of tertiary amines does not proceed in the absence of acetic acid (we noted that their reactions are not photocatalyzed).^[8b] The possible role of acetic acid in our case is to provide H^+ so that CN^- could be more soluble in the solvent, which facilitates nucleophilic attack of CN^- on iminium ion.

Table 2: Conversion and yield of oxidative cyanation of tertiary amines by complex **1**.

Entry	Substrate	R	Product	Conversion, yield [%]
1	5 a	H	6 a	100, 89 ^[a]
2	5 a	H	6 a	100, 50 ^[b]
3	5 a	H	6 a	100, 87 ^[c]
4	5 a	H	6 a	6, n.d. ^[d]
5	5 a	H	6 a	2, n.d. ^[e]
6	5 b	Me	6 b	100, 86 ^[a]
7	5 b	Me	6 b	100, 50 ^[b]
8	5 c	OMe	6 c	100, 84 ^[a]
9	5 c	OMe	6 c	100, 43 ^[b]
10	5 d	Cl	6 d	99, 92 ^[a]
11	5 d	Cl	6 d	100, 27 ^[b]
12	5 e	Br	6 e	100, 82 ^[a]
13	5 e	Br	6 e	100, 33 ^[b]

[a] The substrate (0.107 mmol), NaCN (0.214 mmol), HOAc (0.161 mmol), and catalyst **1** were dissolved in 1.6 mL $\text{CH}_3\text{CN}/\text{CH}_3\text{OH}$ (1:1, v/v). Solvent-saturated O_2 was bubbled into the solution and light ($\lambda > 385$ nm) was focused in front of the quartz cell. After 1.5 h, the solvent was evaporated and the residue was subjected to ^1H NMR analysis. [b] The same reaction conditions as described in [a] except that no acetic acid was added and irradiation time was 3 h. [c] Same reaction conditions as that in [a] except that gaseous HCN was used instead of NaCN/acetic acid. [d] Similar conditions with that in [a] but in the absence of **1**. [e] Similar conditions as in [a] except that the solution was kept in darkness for 24 h. n.d. = not determined.

Complex **1** can also catalyze light-induced generation of hydrogen upon irradiation of a three-component system in a degassed acetonitrile/water mixture comprising **1**, triethanolamine, and $[\text{Co}(\text{dmgH})_2(\text{py})\text{Cl}]$.^[9] Upon irradiation, a bright yellow color, which signified the reduction of Co^{III} to Co^{II} , developed within 30 s. Quenching experiments revealed that oxidative quenching of **1** by $[\text{Co}(\text{dmgH})_2(\text{py})\text{Cl}]$ has a close to diffusion-controlled rate constant of $4.9 \times 10^9 \text{ M}^{-1} \text{ s}^{-1}$. However, reductive quenching with TEOA has not been observed, implying that TEOA acted as a sacrificial donor to reduce the 1^+ generated by oxidative quenching of **1** with $[\text{Co}(\text{dmgH})_2(\text{py})\text{Cl}]$. As depicted in Figure 3, the maximum turnover of hydrogen production was more than 350 after 4 h of irradiation. We also allowed the three-component system in an acetonitrile/water mixture to be irradiated by sunlight. After 4 h, 250 turnovers of hydrogen were obtained. For the photolysis using xenon lamp, we used a glass filter to block the high-energy irradiation ($\lambda < 385$ nm from the xenon lamp), but no such protection was adopted in the experiment when sunlight was used. Light photons with wavelengths ranging from 315 to 385 nm (UV-A) from sunlight are high in energy facilitating the photo-decomposition of **1**. This may account for the reduced amount of hydrogen production. Another well-known method to generate hydrogen from water by light irradiation is to use an electron relay and a hydrogen-generating catalyst.^[8b] Such system involves electron transfer from the photosensitizer to

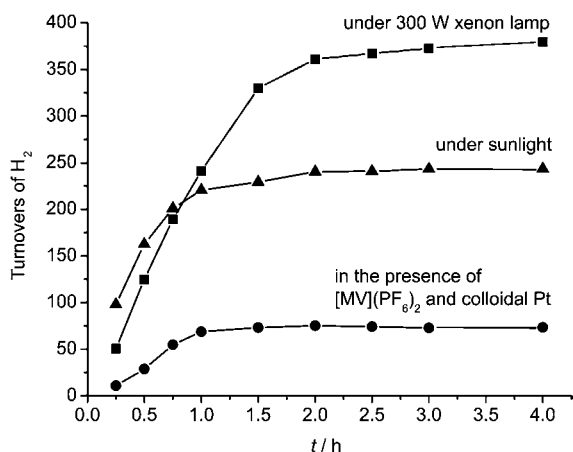


Figure 3. The hydrogen production turnovers of the three-component system (**1**, [Co(dmgH)₂(py)Cl] and triethanolamine) in degassed acetonitrile/water (4:1, v/v) versus time of irradiation by a 300 W Xenon lamp (■), under sunlight (▲), and in the presence of an electron relay (1,1'-dimethyl-4,4'-bipyridinium hexafluorophosphate, [MV](PF₆)₂), colloidal Pt and triethanolamine (●).

the mediator and then to the hydrogen-generating catalyst. When **1** was used as the photosensitizer, the blue color characteristic of the MV⁺ radical (MV²⁺ = 1,1'-dimethyl-4,4'-bipyridinium) developed within 30 s of irradiation. The evolution of hydrogen maintained for one hour and about 75 turnovers were recorded.

In summary, two organogold(III) complexes have been designed to display a long-lived and highly emissive triplet excited state in solutions under ambient conditions. The results of using sunlight and low catalyst loadings for aerobic oxidative C–H bond functionalization and hydrogen production photocatalyzed by complex **1** highlight the richness of organogold(III) photochemistry that has yet to be developed.

Received: November 17, 2011

Revised: January 3, 2012

Published online: February 3, 2012

Keywords: gold · hydrogen production · luminescence · N-heterocyclic carbenes · photooxidation

- [1] a) D. Li, C.-M. Che, H.-L. Kwong, V. W.-W. Yam, *J. Chem. Soc. Dalton Trans.* **1992**, 3325–3329; b) X.-H. Li, L.-Z. Wu, L.-P. Zhang, C.-H. Tung, C.-M. Che, *Chem. Commun.* **2001**, 2280–2281; c) D. M. Roundhill, H. B. Gray, C.-M. Che, *Acc. Chem. Res.* **1989**, 22, 55–61; d) A. J. Esswein, D. G. Nocera, *Chem. Rev.* **2007**, 107, 4022–4047; e) D. A. Nicewicz, D. W. C. MacMillan, *Science* **2008**, 322, 77–80; f) J. M. R. Narayanan, J. W. Tucker, C. R. J. Stephenson, *J. Am. Chem. Soc.* **2009**, 131, 8756–8757.
- [2] a) I. Klimant, M. Köhl, R. N. Glud, G. Holst, *Sens. Actuators B* **1997**, 38, 29–37; b) F. N. Castellano, J. R. Lakowicz, *Photochem. Photobiol.* **1998**, 67, 179–183; c) Q. Zhao, C. H. Huang, F. Y. Li, *Chem. Soc. Rev.* **2011**, 40, 2508–2524.
- [3] a) R. A. Taylor, D. J. Law, G. J. Sunley, A. J. P. White, G. J. P. Britovsek, *Angew. Chem.* **2009**, 121, 6014–6017; *Angew. Chem. Int. Ed.* **2009**, 48, 5900–5903; b) P. W. Du, J. Schneider, P. Jarosz, J. Zhang, W. W. Brennessel, R. Eisenberg, *J. Phys. Chem. B* **2007**, 111, 6887–6894; c) S. C. F. Kui, S. S.-Y. Chui, C.-M. Che, N. Zhu, *J. Am. Chem. Soc.* **2006**, 128, 8297–8309; d) J. A. G. Williams, *Top. Curr. Chem.* **2007**, 281, 205–268.
- [4] C.-W. Chan, W.-T. Wong, C.-M. Che, *Inorg. Chem.* **1994**, 33, 1266–1272.
- [5] a) C. Bronner, O. S. Wenger, *Dalton Trans.* **2011**, 40, 12409–12420; b) W. Lu, K. T. Chan, S.-X. Wu, Y. Chen, C.-M. Che, *Chem. Sci.* **2011**, DOI: 10.1039/c2sc00947a.
- [6] a) K.-H. Wong, K.-K. Cheung, M. C.-W. Chan, C.-M. Che, *Organometallics* **1998**, 17, 3505–3511; b) K. M.-C. Wong, L.-L. Hung, W. H. Lam, N. Zhu, V. W.-W. Yam, *J. Am. Chem. Soc.* **2007**, 129, 4350–4365; c) V. K.-M. Au, K. M.-C. Wong, N. Zhu, V. W.-W. Yam, *J. Am. Chem. Soc.* **2009**, 131, 9076–9085; d) J. J. Yan, A. L.-F. Chow, C. H. Leung, R. W.-Y. Sun, D.-L. Ma, C.-M. Che, *Chem. Commun.* **2010**, 46, 3893–3895; e) J. A. Garg, O. Blacque, T. Fox, K. Venkatesan, *Inorg. Chem.* **2010**, 49, 11463–11472; f) J. A. Garg, O. Blacque, K. Venkatesan, *Inorg. Chem.* **2011**, 50, 5430–5441; g) V. K.-M. Au, K. M.-C. Wong, N. Zhu, V. W.-W. Yam, *Chem. Eur. J.* **2011**, 17, 130–142.
- [7] CCDC 841693 contains the supplementary crystallographic data for this paper. These data can be obtained free of charge from The Cambridge Crystallographic Data Centre via www.ccdc.cam.ac.uk/data_request/cif.
- [8] a) S. Minakata, Y. Ohshima, A. Takemiya, I. Ryu, M. Komatsu, Y. Ohshiro, *Chem. Lett.* **1997**, 311–312; b) K. Yamaguchi, N. Mizuno, *Angew. Chem.* **2003**, 115, 1518–1521; *Angew. Chem. Int. Ed.* **2003**, 42, 1480–1483; c) Y. Maeda, T. Nishimura, S. Uemura, *Bull. Chem. Soc. Jpn.* **2003**, 76, 2399–2403; d) M.-H. So, Y. Liu, C.-M. Ho, C.-M. Che, *Chem. Asian J.* **2009**, 4, 1551–1561; e) T. Naota, H. Takaya, S.-I. Murahashi, *Chem. Rev.* **1998**, 98, 2599–2660; f) S. Singhal, S. L. Jain, B. Sain, *Chem. Commun.* **2009**, 2371–2372; g) X.-Z. Shu, X.-F. Xia, Y.-F. Yang, K.-G. Ji, X.-Y. Liu, Y.-M. Liang, *J. Org. Chem.* **2009**, 74, 7464–7469; h) W. Han, A. R. Ofial, *Chem. Commun.* **2009**, 5024–5026; i) A. G. Condie, J. C. González-Gómez, C. R. J. Stephenson, *J. Am. Chem. Soc.* **2010**, 132, 1464–1465; j) S.-I. Murahashi, *Angew. Chem.* **1995**, 107, 2670–2693; *Angew. Chem. Int. Ed. Engl.* **1995**, 34, 2443–2465; k) G. Jiang, J. Chen, J.-S. Huang, C.-M. Che, *Org. Lett.* **2009**, 11, 4568–4571; l) S.-I. Murahashi, T. Nakae, H. Terai, N. Komiya, *J. Am. Chem. Soc.* **2008**, 130, 11005–11012; m) Z. Li, C.-J. Li, *Eur. J. Org. Chem.* **2005**, 3173–3176; n) Z. Li, C.-J. Li, *J. Am. Chem. Soc.* **2005**, 127, 3672–3673.
- [9] a) X. L. Hu, B. M. Cossairt, B. S. Brunschwig, N. S. Lewis, J. C. Peters, *Chem. Commun.* **2005**, 4723–4725; b) M. Razavet, V. Artero, M. Fontecave, *Inorg. Chem.* **2005**, 44, 4786–4795; c) P. W. Du, K. Knowles, R. Eisenberg, *J. Am. Chem. Soc.* **2008**, 130, 12576–12577.